

Numerical characterization of solar radiation applied to a simplified five parameters diode model of a photovoltaic module in the city of Ngaoundere

Fouakeu-nanfack Gildas Armel ^{1*}, Bikai Jacques ^{2,3}, Nguem Felix Junior ^{1,2,3},
Ndjiya Ngasop ⁴, Edoun Marcel ^{1,3,4,5}

¹ Laboratory of Energetics and Applied Thermal (LETA), National School of Agro-Industrial Sciences (ENSAI),
University of Ngaoundere, Cameroon

² Laboratory of Analysis, Simulation and Testing (LASE), University Institute of Technology (IUT),
University of Ngaoundere, Cameroon

³ Department of Energy Engineering, University Institute of Technology (IUT), University of Ngaoundere, Cameroon

⁴ Department of Electrical Engineering, Energetics and Automation, National School of Agro-Industrial Sciences (ENSAI),
University of Ngaoundere, Cameroon

⁵ Department of Electrical Engineering, University Institute of Technology (IUT), University of Ngaoundere, Cameroon

*Corresponding author E-mail: fouakeunanfack@gmail.com

Abstract

In this paper, another simple and accurate approach to reconstructing the characteristics of a photovoltaic (PV) array exposed to solar radiation has been presented. This approach uses a five-parameter diode model. The approach is based exclusively on the manufacturer's data (three-point method: short-circuit current, open-circuit voltage, maximum power point). To carry out this work, we first carried out a numerical characterization of local solar radiation in the city of Ngaoundere. We then established the mathematical equations describing a solar photovoltaic module, and ran a numerical simulation on Matlab Simulink under standard conditions. The electrical parameters of the photo-voltaic generator and its optimal electrical quantities (current, voltage and power) were analyzed as a function of meteorological variations (temperature, irradiance) and series resistance. The simulation results show that we can achieve a maximum solar irradiance of 1214.9W/m² in the city of Ngaoundere at solar noon. It has been shown that increasing solar irradiance is one of the most productive factors in a PV module. It was also shown that increasing temperature and series resistance considerably reduces the performance of a solar photovoltaic module. This result has enabled us to confirm that these PV cells perform best in a cold, clear-sky environment.

Keywords: Numerical Characterization; Solar Radiation; Photovoltaic Module; Performance.

1. Introduction

Most of the energy consumed today comes from the use of fossil fuels such as oil, coal, natural gas and nuclear power. These resources are becoming increasingly scarce, while the world's energy demands are rising steadily. It is estimated that global reserves will be exhausted around 2030 if consumption is not radically modified, and at most around 2100 if efforts are made on production and consumption (Tumuru et al., 2015). Given that this form of energy covers a large part of current energy production, it is necessary to find another solution to take up the slack. The constraint imposed is to use a low-cost, low-pollution energy source, as environmental protection has become an important issue. Renewable energies, such as solar, wind and water power, are inexhaustible and easily exploitable. Among these renewable energies, solar energy is the most widely exploited in Sahelian zones due to its availability. This energy can be harnessed in two forms, using solar thermal collectors (Fouakeu et al., 2019) or photovoltaic solar panels (Badi et al., 2021). A photovoltaic solar panel is an electrical module comprising photovoltaic cells connected in parallel or series, designed to convert solar radiation into electrical energy. Taking this technology as an example, a surface area of 145,000km² (4% of the surface area of arid deserts) of PV panels would be sufficient to cover the world's entire energy needs (Kassmi et al., 2007). In the latter case, the design, optimization and realization of photovoltaic systems are topical issues, since they will surely lead to better exploitation of solar energy (Zhang et al., 2020). Modeling the latter is therefore a crucial step, and has led to a diversification in the models proposed by different researchers. Their differences lie mainly in the number of diodes, the finite or infinite shunt resistance, the constant or non-constant ideality factor, and the methods for determining the various unknown parameters (Khezzer et al., 2010; Ma et al., 2013a; Orioli and Di Gangi, 2013; Peng et al., 2013, 2014). In the literature, we come across several models whose accuracies remain dependent on the mathematical modeling of the various intrinsic physical phenomena involved in the power generation process. Most of the literature uses the equivalent four-parameter model based on mathematical modeling of the voltage-current curve (Khezzer et al., 2010). But this model is simpler and less accurate (Ghani et al., 2013; Ghani and

Duke, 2011). The aim of our work is to reconstruct the characteristics of a photovoltaic panel from one of these cells, and to model and simulate it in order to improve its electrical performance. To do so, we will use the equivalent five-parameter model (Dongue et al., 2012; Li et al., 2013; Ma et al., 2013a, 2013b; Orioli and Di Gangi, 2013; Satapathy et al., 2018; Boussaibo et al., 2024), which offers better accuracy compared to the four-parameter model and is less complex compared to the double diode model (Cuce and Cuce, 2012; Ghani et al., 2013). Subsequently, the characteristic curves $I_{pv}(V)$ and $P_{pv}(V)$ were reconstructed and plotted.

2. Materials and methods

2.1. Materials

The monocrystalline photovoltaic solar module is being studied in Cameroon, in the Adamaoua region, mainly in the town of Ngaoundere (Latitude: 7.338149 and Longitude: 13.56683). This module is dark and black in color. It is covered by a thin glass plate. The cells are encapsulated in a waterproof coating that protects them from water and water vapor. The photovoltaic solar module weighs 20.5 kg, has a length (L) of 1769 mm, a width (W) of 1052 mm and a thickness (e) = 35 mm. The following figure shows the photovoltaic solar module studied in this work.

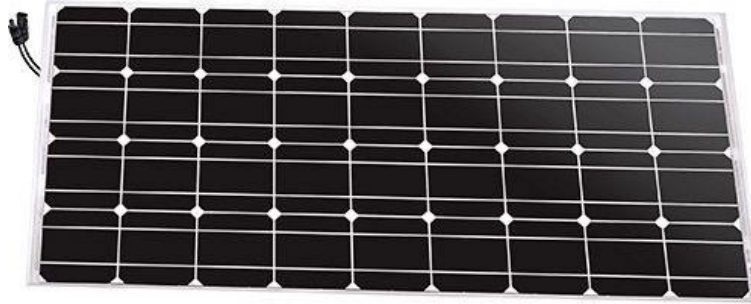


Fig. 1: Physical Model of the Photovoltaic Module.

2.2. Modeling

2.2.1. Solar radiation modelling

To calculate global solar irradiance G , we used the approach proposed by Jannot (2003). The declination δ is determined by the following expression:

$$\delta = 23.45 \sin 0.986^\circ (j + 284) \quad (1)$$

The hour angle is defined by :

$$w = 15^\circ (TS - 12) \quad (2)$$

The height h of the Sun is deduced by :

$$\sinh = \sin L * \sin \delta + \cos L * \cos \delta * \cos w \quad (3)$$

The azimuth a is deduced by:

$$\sin a = \frac{\cos \delta * \sin w}{\cosh} \quad (4)$$

The modulus w_1 of the hour angle at sunrise is obtained by writing $\sin(h) = 0$, which leads to leads to :

$$\cos w_1 = -\tan L * \tan \delta \quad (5)$$

Solar time at sunrise is therefore expressed as :

$$(TS)_1 = 12 - \frac{w_1}{15} \quad (6)$$

The solar flux I received on the surface permanently oriented towards the sun and which therefore receives solar radiation at normal incidence is expressed by :

$$I = 1370 \exp\left(-\frac{TL}{0.9 + 9.4 \sinh}\right) \quad (7)$$

Where TL is the Link disturbance factor calculated by :

$$TL = 2.4 + 14.6\beta + 0.4(1 + 2\beta)\ln(p_v) \quad (8)$$

Direct radiation D is deduced by :

$$D = I \sin(h) \quad (9)$$

The diffuse radiation S is calculated by the correlation :

$$S = 54.8\sqrt{\sin(h)} \left[TL - 0.5 - \sqrt{\sin(h)} \right] \quad (10)$$

Global radiation G is determined by :

$$G = S + D \quad (11)$$

2.2.2. Modeling a PV module

A PV module consists of a number of solar cells connected in series and parallel to achieve the desired voltage and current levels. A solar panel cell is essentially a p-n semiconductor junction. When exposed to light, a direct current is generated. For simplicity, the single-diode model shown in figure 2 is used in this document. This model offers a good compromise between simplicity and accuracy with its basic structure. The equivalent circuit of the general model consists of a photocurrent (I_{ph}), a diode, a parallel resistor (R_p) expressing a leakage current and a series resistor (R_s) due to contacts between semiconductors and metal parts.

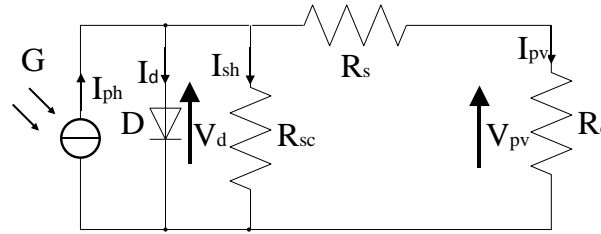


Fig. 2: Model of A Photovoltaic Solar Cell.

The one-diode model has the advantage of simplicity. It provides the static behavior of a PV cell under bias. From the equivalent circuit, the current generated by the PV cell is (Zhang et al., 2020; Kadeval and Patel, 2021).

$$I_{pv} = I_{ph} - I_d - I_{sh} \quad (12)$$

Where I_{ph} is the current generated by the light, I_{sh} is the current flowing through the parallel resistor and I_d is the diode current which is proportional to the saturation current. The diode current (I_d) can be expressed by the following expression (Bi et al., 2017):

$$I_d = I_s \left[\exp \left(\frac{q(V_{pv} + R_s I_{pv})}{kT_c A} \right) - 1 \right] \quad (13)$$

Where I_s is the reverse saturation current in amperes (A), q is the electron charge (1.6×10^{-19} C), k is Boltzmann's constant (1.38×10^{-23} J/K), T_c is a cell temperature ($^{\circ}$ C), A is the diode's ideal factor and R_s is a series resistor (Ω). Applying the mesh law, the current (I_{sh}) flowing through the parallel resistor can be represented by the following expression:

$$I_{sh} = \frac{V_{pv} + R_s I_{pv}}{R_{sh}} \quad (14)$$

The equation for the current generated by the photovoltaic cell becomes (Boussaibo et al., 2024):

$$I_{pv} = I_{ph} - I_s \left[\exp \left(\frac{q(V_{pv} + R_s I_{pv})}{kT_c A} \right) - 1 \right] - \frac{V_{pv} + R_s I_{pv}}{R_{sh}} \quad (15)$$

The photon current (I_{ph}) depends mainly on the solar irradiance and the operating temperature of the cell, which is described by the following equation (Satapathy et al., 2018):

$$I_{ph} = \frac{G}{G_{ref}} \left[I_{sc} + k_i (T_c - T_{ref}) \right] \quad (16)$$

Where I_{sc} is the short-circuit current of the cell at 25°C and $1000\text{W}/\text{m}^2$, K_i is the temperature coefficient of the short-circuit current of the cell, T_{ref} is the reference temperature of the cell in $^{\circ}\text{C}$, G is the insolation in W/m^2 and G_{ref} : the reference insolation of the cell in W/m^2 . On the other hand, cell saturation current varies with cell temperature, which is described as follows (Hysa, 2019):

$$I_s = I_{rs} \left(\frac{T_c}{T_{ref}} \right)^3 \exp \left[\frac{qE_g \left(\frac{1}{T_{ref}} - \frac{1}{T_c} \right)}{kA} \right] \quad (17)$$

Where I_{rs} is the reverse saturation current of the cell at a reference temperature and solar irradiation, E_g is the gap energy of the semiconductor used in the cell in electronvolt (eV) and A is the ideal factor which depends on the PV technology. The inverse saturation current is given by the following equation (Ghani and Duke, 2011):

$$I_{rs} = \frac{I_{sc}}{\exp \left(\frac{qV_{oc}}{N_s A k T_c} \right) - 1} \quad (18)$$

Where N_s is the number of cells in series in a PV module, I_{sc} is the short-circuit current and V_{oc} is the open-circuit voltage. The equivalent circuit for a solar module with N_s cells in series and N_p cells in parallel is shown in Figure 3.

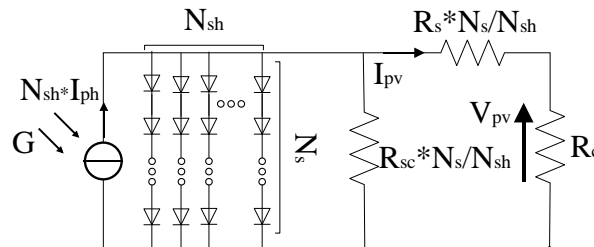


Fig. 3: Equivalent Model of A Photovoltaic Solar Module.

The terminal equation for the current and voltage of a PV module becomes the following (Essakhi, 2019; Boussaibo et al., 2024):

$$I_{pv} = R_{sh} I_{ph} - R_{sh} I_s \left[\exp \left(\frac{q \left(\frac{V_{pv}}{N_s} + \frac{R_s I_{pv}}{N_{sh}} \right)}{k T_c A} \right) - 1 \right] - \frac{N_{sh} V_{pv} + R_s I_{pv}}{R_s} \quad (19)$$

The terminal equation for the power and voltage of a PV module is described with the following expression (Robinson et al., 2020):

$$P_{pv} = V_{pv} I_{pv} = V_{pv} \left(R_{sh} I_{ph} - R_{sh} I_s \left[\exp \left(\frac{q \left(\frac{V_{pv}}{N_s} + \frac{R_s I_{pv}}{N_{sh}} \right)}{k T_c A} \right) - 1 \right] - \frac{N_{sh} V_{pv} + R_s I_{pv}}{R_s} \right) \quad (20)$$

PV module current and power were simulated under the influence of illuminance, wall temperature and cell series resistance as a function of PV module voltage. The following table shows the simulation parameters of the PV module under standard conditions (optical mass: AM 1.5).

Table 1: Photovoltaic Module Characteristics

Module parameters	Symbols	Values
Power rating	P_n	190 W
MPP voltage	V_{mp}	36,14 V
Short circuit current	I_{sc}	5,69 A
Open circuit voltage	V_{oc}	43,66 V
Number of cells in series	N_s	72
Number of cells in parallel	N_{sh}	1
Ideal diode factor	A	1,2
Temperature coefficient of short-circuit current	k_i	0.04%
Parallel resistance	R_{sh}	300 Ω
Solar radiation	G	1000 – 800 – 600 – 400 – 200 W/m^2
Cell temperature	T	25 – 35 – 45 – 55 – 65 $^{\circ}\text{C}$
Series resistance	R_s	0.001 - 0.011 - 0.021 - 0.031 - 0.041 Ω

2.2.3. Methods of resolution

The solar radiation equations were solved simultaneously using Matlab 2014 software. The solar photovoltaic module was simulated with the Matlab Simulink interface under the influence of irradiance, wall temperature and cell series resistance. The following figure 4 shows the block diagram of the PV cell in Matlab-Simulink.

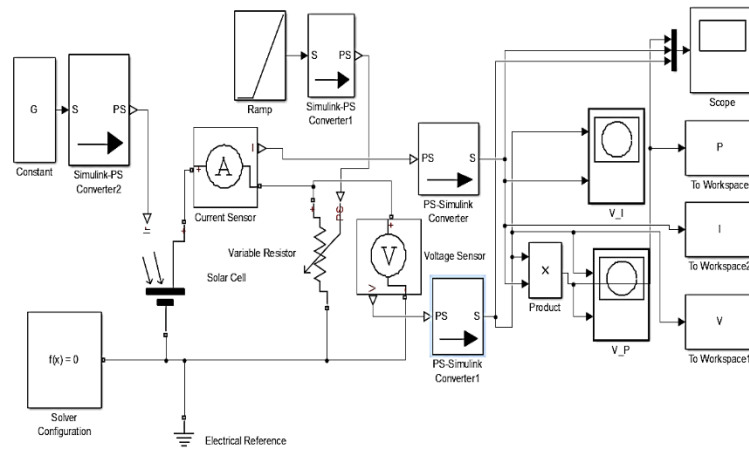


Fig. 4: PV Module Block Diagram in Matlab-Simulink.

3. Results and discussion

3.1. Characterization of daily solar radiation

Figure 5 shows the evolution of predicted diffuse (S), direct (D) and global (G) solar radiation as a function of time. Analysis of figure 4 shows that the three curves evolve in a similar bell-shaped pattern. This shows the increase and decrease in sunshine during the day. It can be seen from this figure that at 13:00 min, global radiation reached a maximum value of 1214.907 W/m². This solar flux value proves the sufficiency of solar irradiance for solar collector performance evaluation, since the ASHRAE (American Society of Heating, Refrigerating and Air-Conditioning Engineers standard) requires that, for solar collector efficiency tests, solar irradiance must be above 630 W/m² (Fouakeu et al., 2019).

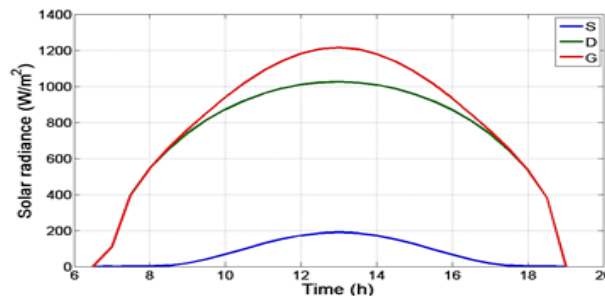


Fig. 5: Solar Radiation Profile.

3.2. Characterization of the photovoltaic solar module

3.2.1. Influence of solar radiation

Figure 6 below shows the evolution of photovoltaic electric current as a function of electric voltage $I_{pv}(V)$ under the influence of solar irradiance. It can be seen that when solar irradiance increases by 200 W/m², current intensity increases by 1.14 A. However, the voltage increases by 3.53V when solar irradiance rises from 200W/m² to 1000W/m². This result reassures us that the PV module's electric current is highly dependent on solar irradiance. This result is similar to that of Satapathy et al. (2018), Badi et al. (2021) et Boussaibo et al. (2024), who characterized a PV module with solar irradiance varying from 100 W/m² to 1000 W/m².

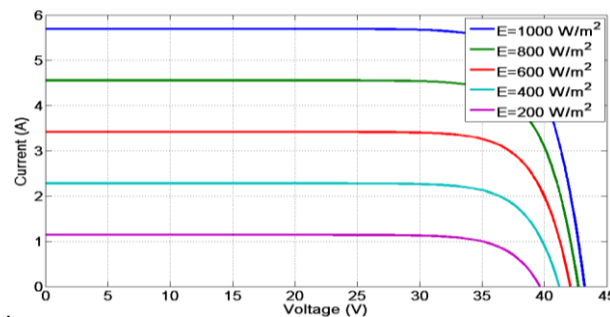


Fig. 5: $I_{pv}(V)$ Characteristics of A PV Module for Different Solar Irradiances ($T=25^{\circ}C$ And $R_s=0.001\Omega$).

Figure 7 shows the evolution of the PV module's electrical power as a function of the electrical voltage $P_{pv}(V)$ under the influence of solar irradiance. It can be seen that as solar irradiance increases, the PV module produces more electrical power. It is also observed that when irradiance increases by 200 W/m^2 , the maximum PV power increases by 36 W . This result reassures us that the PV module's electrical power is highly dependent on solar irradiance. Similar results were observed in the work of Bi et al. (2017), Satapathy et al. (2018) et Badi et al. (2021), who obtained an increase in power of 37 W when solar irradiance increased by 200 W/m^2 .

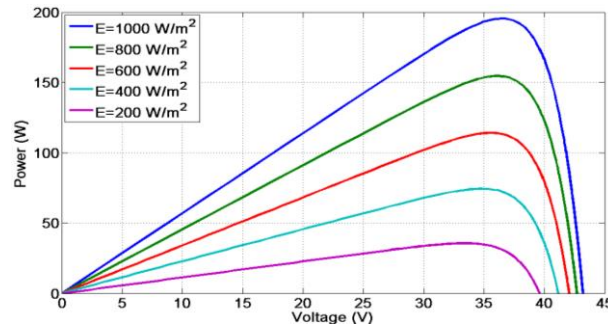


Fig. 6: $P_{pv}(V)$ Characteristics of A PV Module for Different Solar Irradiances ($T=25^\circ\text{C}$ and $R_s=0.001\Omega$).

3.2.2. Influence of cell temperature

Figure 8 shows the evolution of the photovoltaic electric current as a function of the electric voltage $I_{pv}(V)$ under the influence of cell temperature. It can be seen that when the cell temperature increases by 10°C , the current intensity increases very slightly, resulting in a pronounced decrease of 1.35 volts in the PV module voltage. This result is similar to that of Satapathy et al. (2018), Azem and Klemo (2019) et Kadeval and Patel (2021) who characterized a PV module under solar radiation of 1000 W/m^2 .

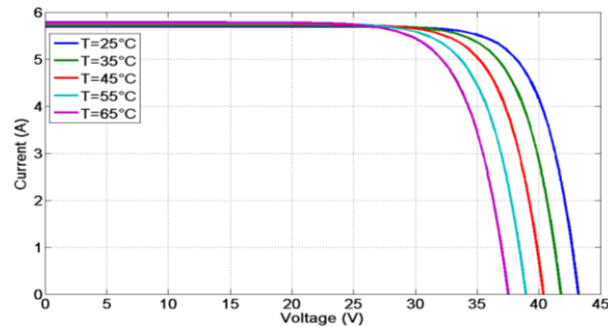


Fig. 7: $I_{pv}(V)$ Characteristics of A PV Module for Different Temperatures ($G=1000\text{W/M}^2$ and $R_s=0.001\Omega$).

The following figure 9 shows the evolution of the PV module's electrical power as a function of the electrical voltage $P_{pv}(V)$ under the influence of cell temperature. It can be seen that the maximum PV power is 196.989 188.889 180.789 172.321 and 164.589 W for cell temperatures of 25 , 35 , 45 , 55 and 65°C respectively. These profiles show that as cell temperature increases, the PV module produces less electrical power. This result reassures us that increasing cell temperature significantly reduces PV performance. Satapathy et al. (2018), Azem and Klemo (2019) et Kadeval and Patel (2021) had obtained similar results by characterizing a PV module under solar radiation of 1000 W/m^2 .

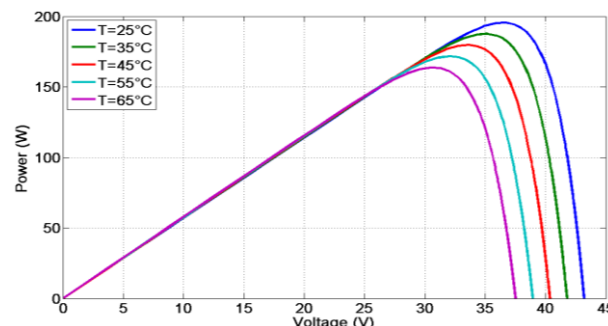


Fig. 8: $P_{pv}(V)$ Characteristics of A PV Module for Different Temperatures ($G=1000 \text{ W/M}^2$ and $R_s=0.001 \Omega$).

3.2.3. Influence of cell series resistance

Figure 10 shows the evolution of photovoltaic electric current as a function of electric voltage under the influence of the cell's series resistance. It can be seen that the series resistance affects the slope of the characteristic in the area where the photodiode behaves as a voltage generator. It does not affect the open-circuit voltage or the short-circuit current. This result is similar to that of (Hysa, 2019), who characterized a PV module under solar radiation of 1000 W/m^2 .

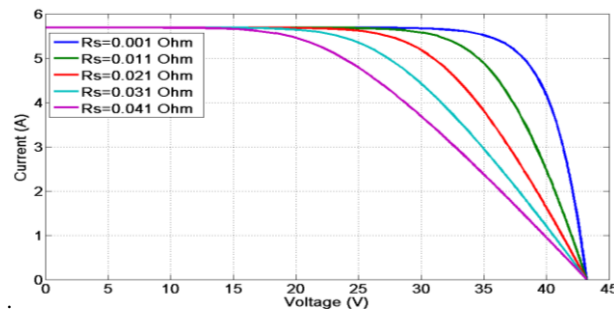


Fig. 9: $I_{pv}(V)$ Characteristics of A PV Module for Different Series Resistances ($G=1000 \text{ W/M}^2$ and $T=25^\circ\text{C}$).

The following figure 11 shows the evolution of the PV module's electrical power as a function of the electrical voltage under the influence of the series resistance. It is observed that the maximum power of the PV module is 195.971; 175.458; 156.044; 136.63 and 119.78 respectively for series resistances of 1 m Ω , 11 m Ω , 21 m Ω , 31 m Ω and 41 m Ω . Increasing the series resistance results in a decrease in the slope of the power curve. It is also noted that as the series resistance of the cell increases, the PV module produces less electrical power. This result is similar to the work of Ghani and Duke (2011) et Hysa (2019) who characterized a PV module under solar radiation of 1000 W/m 2 .

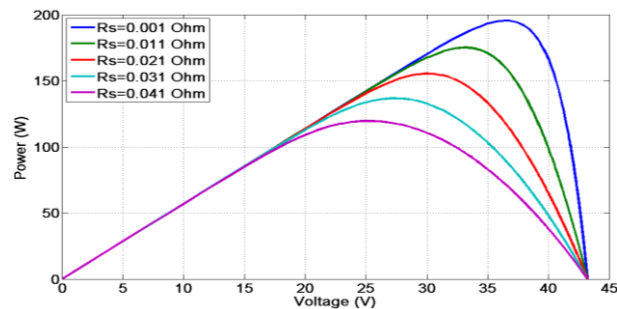


Fig. 10: $P_{pv}(V)$ Characteristics of A PV Module for Different Resistances ($G=1000\text{W/M}^2$ and $T=25^\circ\text{C}$).

4. Conclusion

the aim of this work was to present another simple and accurate approach to reconstructing the characteristics of a photovoltaic generator exposed to solar radiation. this approach uses a five-parameter diode model. to achieve this, we first performed a numerical characterization of the local solar radiation. we then established the mathematical equations describing a solar photovoltaic module and ran a numerical simulation on Matlab simulink under standard conditions. the electrical parameters of the photovoltaic generator were analyzed as a function of weather variations and series resistance. the results of the simulation showed that we could obtain maximum sunshine of 1214.9 w/m 2 in the city of Ngaoundere. it has been shown that increasing solar irradiance is one of the most productive factors in a pv module. it was also shown that increasing temperature and series resistance considerably reduces the performance of a solar photovoltaic module. this result has enabled us to confirm that these pv cells perform best in a cold, clear-sky environment.

Acknowledgement

The authors would like to thank the head of the Doctoral Training Unit – Applied Physics and Engineering of the National School of Agro-Industrial Sciences (ENSAI) of the University of Ngaoundere for the material support he provided during our research work.

References

- [1] Azem, H., Klemo, M., 2019. Modeling and simulation of photovoltaic cell with matlab for different temperature and different solar radiation. *Interdisciplinary Journal of Research and Development* 6, 44–44. <https://doi.org/10.56345/ijrdv6n204>.
- [2] Badi, N., Khasim, S., Al-Ghamdi, S.A., Alatawi, A.S., Ignatiev, A., 2021. Accurate modeling and simulation of solar photovoltaic panels with simulink-MATLAB. *J Comput Electron* 20, 974–983. <https://doi.org/10.1007/s10825-021-01656-0>.
- [3] Bi, B.E.B., GBAHA, P., SAKO, M.K., KOFFI, M.P.E., 2017. Modélisation et simulation d'un panneau solaire photovoltaïque par utilisation de la fonction W de Lambert et de Matlab-Simulink. *Afrique SCIENCE* 13, 18–28.
- [4] Boussaibo, A., Alphonse, S., Stephane, N.N., Goron, D., Duvalier, P.A., Kitmo, 2024. Modeling of a photovoltaic drip irrigation system for an offseason crop: case of onion cultivation in PITO (North Cameroon). *International Journal of Engineering & Technology* 13, 1–12.
- [5] Cuce, P.M., Cuce, E., 2012. A novel model of photovoltaic modules for parameter estimation and thermodynamic assessment. *International Journal of Low-Carbon Technologies* 7, 159–165. <https://doi.org/10.1093/ijlct/ctr034>.
- [6] Dongue, S.B., Njomo, D., Tamba, J.G., Ebengai, L., 2012. Modeling of electrical response of illuminated crystalline photovoltaic modules using four-and five-parameter models. *International Journal of Emerging Technology and Advanced Engineering* 2, 612–619.
- [7] Essakhi, H., 2019. modélisation et simulation d'un module photovoltaïque. LASIME, ESTA Université Ibn Zohr, BP 33.
- [8] Fouaqueu, N.G.A., Tetang, F.A., Edoun, M., Kuitche, A., Zeghmami, B., 2019. A contribution to a numerical characterization of the thermal transfers in a saw tooth solar collector. *International Journal of Thermal Technologies* 9, 200–206. <https://doi.org/10.14741/ijtt/v.9.3.1>
- [9] Ghani, F., Duke, M., 2011. Numerical determination of parasitic resistances of a solar cell using the Lambert W-function. *Solar Energy* 85, 2386–2394. <https://doi.org/10.1016/j.solener.2011.07.001>.
- [10] Ghani, F., Duke, M., Carson, J., 2013. Numerical calculation of series and shunt resistances and diode quality factor of a photovoltaic cell using the Lambert W-function. *Solar Energy* 91, 422–431. <https://doi.org/10.1016/j.solener.2012.09.005>.
- [11] Hysa, A., 2019. Modeling and simulation of the photovoltaic cells for different values of physical and environmental parameters. *Emerging Science Journal* 3, 395–406. <https://doi.org/10.28991/esj-2019-01202>.

- [12] Jannot, Y., 2003. Thermique solaire. p30-p70, October.
- [13] Kadeval, H.N., Patel, V.K., 2021. Mathematical modelling for solar cell, panel and array for photovoltaic system. *Journal of Applied and Natural Science* 13, 937–943. <https://doi.org/10.31018/jans.v13i3.2529>.
- [14] Kassmi, K., Hamdaoui, M., Oliv  , F., 2007. Conception et mod  lisation d’un syst  me photovolta  que adapt   par une commande MPPT ana-logique. *Journal of Renewable Energies* 10, 451–462. <https://doi.org/10.54966/jreen.v10i4.749>.
- [15] Khezzar, R., Zereg, M., Khezzar, A., 2010. Comparaison entre les diff  rents mod  les   lectriques et d  termination des param  tres de la caract  ristique IV d’un module photovolta  que. *Journal of Renewable Energies* 13, 379–388. <https://doi.org/10.54966/jreen.v13i3.206>.
- [16] Li, Y., Huang, W., Huang, H., Hewitt, C., Chen, Y., Fang, G., Carroll, D.L., 2013. Evaluation of methods to extract parameters from current–voltage characteristics of solar cells. *Solar Energy* 90, 51–57. <https://doi.org/10.1016/j.solener.2012.12.005>.
- [17] Ma, J., Man, K.L., Ting, T.O., Zhang, N., Guan, S.-U., Wong, P.W., 2013a. Approximate single-diode photovoltaic model for efficient I-V characteristics estimation. *The Scientific World Journal* 2013. <https://doi.org/10.1155/2013/230471>.
- [18] Ma, J., Ting, T.O., Man, K.L., Zhang, N., Guan, S.-U., Wong, P.W., 2013b. Parameter estimation of photovoltaic models via cuckoo search. *Journal of applied mathematics* 2013. <https://doi.org/10.1155/2013/362619>.
- [19] Orioli, A., Di Gangi, A., 2013. A procedure to calculate the five-parameter model of crystalline silicon photovoltaic modules on the basis of the tabular performance data. *Applied energy* 102, 1160–1177. <https://doi.org/10.1016/j.apenergy.2012.06.036>.
- [20] Peng, L., Sun, Y., Meng, Z., 2014. An improved model and parameters extraction for photovoltaic cells using only three state points at stand-ard test condition. *Journal of power Sources* 248, 621–631. <https://doi.org/10.1016/j.jpowsour.2013.07.058>.
- [21] Peng, L., Sun, Y., Meng, Z., Wang, Y., Xu, Y., 2013. A new method for determining the characteristics of solar cells. *Journal of power sources* 227, 131–136. <https://doi.org/10.1016/j.jpowsour.2012.07.061>.
- [22] Robinson, N., Justus, S., Elijah, A., Nicodemus, O., 2020. A fast and accurate analytical method for parameter determination of a photovoltaic system based on manufacturer’s data. *Journal of Renewable Energy* 2020, 1–18. <https://doi.org/10.1155/2020/7580279>.
- [23] Satapathy, L.M., Harshita, A., Saif, M., Dalai, P.K., Jena, S., 2018. Comparative analysis of boost and buck-boost converter in photovoltaic power system under varying irradiance using MPPT, in: 2018 Second International Conference on Inventive Communication and Computational Technologies (ICICCT). IEEE, pp. 1828–1833. <https://doi.org/10.1109/ICICCT.2018.8473222>.
- [24] Tummuru, N.R., Mishra, M.K., Srinivas, S., 2015. Dynamic energy management of renewable grid integrated hybrid energy storage system. *IEEE Transactions on Industrial Electronics* 62, 7728–7737. <https://doi.org/10.1109/TIE.2015.2455063>.
- [25] Zhang, C., Zhang, Y., Su, J., Gu, T., Yang, M., 2020. Performance prediction of PV modules based on artificial neural network and explicit analytical model. *Journal of Renewable and Sustainable Energy* 12. <https://doi.org/10.1063/1.5131432>.